

GRIDMAP-Based Modeling and MIPSO-Driven Optimization for the Placement and Relocation of Reclosers, Sectionalizers, Fuses, Remote-Controlled Switches, and Manual Switches in Distribution Grids

Mehdi Mohammadian Mehr^a , Hossein Farzin^{a*} 

a. Faculty of Engineering, Department of Electrical Engineering, Shahid Chamran University of Ahvaz, Ahvaz, Iran, 61357-43337.

* Corresponding author: Farzin@scu.ac.ir

Abstract

This paper introduces a framework for the optimal allocation of protection and control devices including reclosers, sectionalizers, fuses, remote-controlled switches, and manual switches in power distribution systems. Central to this study is the development of the GRIDMAP model, a scalable, matrix-based representation of the distribution network topology. GRIDMAP enables detailed modeling of complex grid structures, supports both permanent and temporary fault analysis, and integrates real-world operational constraints such as device relocation and load growth. Building upon this modeling foundation, a Modified Particle Swarm Optimization (MIPSO) algorithm is implemented to solve the allocation problem. The algorithm leverages GRIDMAP's structure to evaluate candidate locations efficiently, apply relocation strategies for existing devices, and minimize both installation and customer interruption costs. The MIPSO model outperforms ACO and ICA in cost and speed, shows stable results over 10 runs, and sensitivity analysis highlights the trade-off between equipment quality, total cost, and computation time. Notably, the model allows the relocation of existing equipment within the optimization process, and can be extended to other metaheuristic algorithms with ease. The proposed method is validated through four distinct scenarios on a modified IEEE 69-bus distribution system. Overall, GRIDMAP proves to be a robust and adaptable tool for advanced distribution grid planning and reliability enhancement.

Keywords : Optimal Switch Allocation, Protection and Control Devices, Mixed-Integer Particle Swarm Optimization (MIPSO), Device Relocation, Distribution Grid Planning, Graph-based Representation and Integrated Distribution Modeling for Analysis and Planning (GRIDMAP)

Nomenclature	
Indices and Sets	
k	Identifier for the type of load (R: Residential, C: Commercial, I: Industrial)
n	Number of nodes in the main branch
m	Number of nodes in the largest sub-branch
t	Duration of study in years
Lr	Annual load growth rate
(i, ii)	Index counters for row, and column in the branch information matrix
(j, jj)	Index counters for row, and column in the load information matrix
Parameters and Constants	
$IC_{(i,ii)}^{(Re/fu/sec/RCS/MS)}$	Initial purchase cost of switches (currency unit)
α	Inflation rate
d	Interest Rate
$MC_{(i,ii)}^{(Re/fu/sec/RCS/MS)}$	Maintenance cost of devices (currency unit)
$RC_{(i,ii)}^{(Re/fu/sec/RCS/MS)}$	Relocation cost of devices (currency unit)
$\lambda_{(i,ii)}^{(P/T)}$	Annual permanent and temporary failure rates of branches (failures/year) or (f/y)
$load_{(j,jj)}$	Average requested load (kWh)
$cdf_{(j,jj,k)}$	Customer loss cost (\$ per kWh)
Variables and Functions	
C^{eq}	Total investment cost of devices
C^{Total}	Expected interruption cost for devices
C^{PS}	Investment cost for protective devices
C^{CS}	Investment cost for control devices
C^P	interruption cost due to permanent failure
C^T	interruption cost due to temporary failure
$X_{(i,ii)}^{(Re/fu/sec/RCS/MS)}$	A binary variable that determines which switch is installed at the candidate point coordinates
$RX_{(i,ii)}^{(Re/fu/sec/RCS/MS)}$	A binary variable that determines which switch is relocation at the candidate point coordinates
$IX_{(i,ii)}^{(Re/fu/sec/RCS/MS)}$	A binary variable that determines which switch should be purchased at which coordinates.
$dr_{(j,jj)}^{(P/T)}$	Duration of grid interruption due to permanent and temporary failures for various loads (hours) or (h)

1. Introduction

1.1 Motivation

The increasing demand for reliable and efficient power distribution systems has necessitated the implementation of advanced protective and control devices such as Reclosers (Re), Fuses (Fu), sectionalizers(Sec), Remote-Controlled Switches (RCS), and Manual Switches (Ms). These devices play a critical role in safeguarding electrical grids, preventing cascading failures, and ensuring the stability of power supply [1]. As the complexity of power distribution systems grows, driven by factors such as the integration of renewable energy sources and rising consumer demand, the optimization of these protective devices becomes essential [2-4]. This paper explores the optimal allocation of these protective devices, focusing on enhancing the reliability of power distribution grids [5-7]. The reliability of power distribution grids is of paramount importance for utility companies and consumers alike [8-10]. Frequent interruptions and system failures not only disrupt service but also incur significant economic costs and affect customer satisfaction [11]. In today's competitive energy market, maintaining high reliability is crucial for utilities to retain customers and meet regulatory standards [12, 13]. By focusing on the optimal allocation of protective devices, this research aims to contribute to the development of smarter, more resilient power distribution systems capable of adapting to evolving demands and challenges [14]. To address the modeling and optimization needs of modern grids, this study introduces the GRIDMAP framework (Graph-based Representation and Integrated Distribution Modeling for Analysis and Planning). GRIDMAP offers a scalable and flexible representation of distribution grids by translating electrical topology and operational data into a structured matrix-based format. This structured modeling approach enables seamless integration with metaheuristic optimization algorithms, supporting both analytical studies and strategic planning in large-scale distribution systems. A key advantage of GRIDMAP is its adaptability it can be combined with various heuristic and metaheuristic methods. In this study, the Mixed-Integer Particle Swarm Optimization (MIPSO) algorithm is utilized in combination with GRIDMAP. This approach is used to solve a real-world optimal allocation problem involving protection and control devices in the modified IEEE 69-bus test system. The model not only considers installation and interruption costs, but also incorporates device relocation scenarios, offering a more realistic and cost-effective solution that reflects actual utility

constraints. By supporting such complex functionalities, GRIDMAP addresses the limitations of conventional models and enhances the ability to plan and operate smarter, more resilient distribution systems.

1.2 Literature Survey

Building upon these advancements, the present study introduces the GRIDMAP model and a MIPSO-based optimization framework, addressing key gaps in scalability, device relocation, and integrated fault analysis, while aligning with recent trends in topology-aware, DG-integrated, and metaheuristic-based distribution system planning. Reference [15] highlights the importance of precise radiality constraint modeling for fast and accurate network reconfiguration. In [16], an efficient framework is introduced for optimal DG allocation under variable loads to minimize losses. Reference [17] incorporates temperature-dependent load behavior into reconfiguration models to better reflect real-world conditions. Fuel cell performance and recovery phenomena are modeled in [18] using improved LSTM networks, while [19] proposes a rolling prediction framework for long-term fuel cell health estimation. Reference [20] introduces a multi-strategy optimization algorithm (MS-TSO) for accurate PEMFC voltage model parameter estimation. In [21], a MILP-based method is developed for optimal switch and breaker placement under varying load levels. The switch allocation problem with DG is tackled in [22] using a memetic algorithm applied to large-scale networks. Reference [23] presents a reconfiguration method for active distribution networks with SOPs and protection constraints. Lastly, [24] proposes a graph-based approach for optimal switch placement in interconnected microgrids, improving both scalability and reliability.

The optimal allocation of sectionalizing and RCS plays a crucial role in improving grid reliability. Previous studies have shown that while incorporating malfunction probabilities and applying Markov chains can enhance the accuracy of the solution, their impact on reducing costs is relatively limited [25]. Additionally, the integration of distribution automation, such as tie switches and Re, has been found effective in minimizing downtime and enhancing overall system performance [26]. A model for the optimal allocation of disconnect switches, considering both manual and RCS, as well as tie switches, has been successfully

applied to reliability enhancement [27]. Furthermore, a novel solution method has been proposed that reformulates the deployment of manual and automatic switches as a mixed integer linear programming (MILP) problem, demonstrating that fewer switches can yield better reliability outcomes [28]. Protection and control systems, including fault indicators and sectionalizing switches, are essential for reducing downtime and improving service quality within distribution grids [29]. The inclusion of M in allocation strategies also significantly contributes to the optimal positioning of protection devices, thus enhancing grid reliability [30]. Moreover, integrating long-term load forecasting (LTLF) into switch allocation models has proven to refine demand projections, further improving the overall solution [31]. The role of distributed generation (DG) in switch allocation is also vital, as it enhances system reliability and reduces energy not supplied (ENS) during faults [32, 33].

The use of genetic algorithms and Particle Swarm Optimization (PSO) techniques has demonstrated success in optimizing switch allocation in real-world distribution systems, delivering effective and practical solutions [32]. Additionally, Reference [34] highlights the use of an improved gravitational search algorithm (IGS) to optimize the allocation of protective switches, aiming to minimize interruption time and energy loss, thus enhancing the system reliability. Finally, relocating existing equipment within the grid can significantly lower both installation and maintenance costs while optimizing the use of current infrastructure [1]. Building on the insights gained, this paper incorporates MIPSO algorithms into the optimal allocation framework. This integration addresses existing gaps and enhances the process of determining optimal locations for protection and control devices in power distribution grids. A summary of these approaches is presented in Table 1. Recent studies have underscored the advantages of MIPSO algorithms in effectively solving the optimization problems, thus making them highly suitable for the present research. These algorithms have been successfully applied in a variety of contexts, including grid reconfiguration and fault management, demonstrating their ability to efficiently navigate large solution spaces and provide optimal solutions [35, 36].

Table 1: Comparison of Recent research on reliability-based switch placement

Despite the significant progress made in previous research, many existing methods remain limited in their ability to model complex, large-scale grids under realistic operational constraints. In contrast, this study leverages the GRIDMAP modeling framework, which provides a powerful and adaptable structure for representing the topology and behavior of actual distribution systems. This model not only supports detailed analysis of protective and control equipment allocation but also facilitates integration with advanced metaheuristic algorithms such as MIPSO. As demonstrated in this work, the combination of GRIDMAP and MIPSO enables efficient handling of device relocation, interruption duration analysis, and real-world constraints.

1.3 Contributions

This paper presents a novel GRIDMAP modeling framework for the optimal allocation of protection and control devices, including Re, Sec, Fu, RCS, and MS in power distribution systems. The framework seamlessly integrates with metaheuristic algorithms like PSO to optimize device placement and relocation in real-world grids, such as the modified IEEE 69-bus system. GRIDMAP's innovation lies in its ability to model both new and existing equipment, enabling cost-efficient, reliable solutions while addressing real-world constraints and dynamic grid needs. The main contributions of this study are as follows:

1. The proposed Model-Based Optimization Framework is built on the GRIDMAP model, which transforms the grid into a structured, matrix-based representation. This facilitates clear analysis of node-to-load relationships, enabling the effective application of optimization algorithms to real-world grid conditions. The matrix-based architecture of GRIDMAP allows for accurate modeling of complex grid topologies, including main feeders and multiple branched sub-feeders, ensuring scalability for large-scale grids. Furthermore, the structured design of GRIDMAP is not limited to the MIPSO algorithm used in this study. Its standardized representation of devices, loads, and grid topology ensures compatibility with various metaheuristic and classical optimization methods. This makes GRIDMAP a reusable and extensible platform for future research and practical applications.

2. Unlike traditional methods, the GRIDMAP model incorporates a native mechanism for device relocation. Through its coordinate-based structure, the model identifies whether a proposed device is already installed at the correct location, requires repositioning, or needs to be newly installed allowing for a realistic representation of equipment movement and reducing redundant installation costs.
3. The enhanced Metaheuristic Algorithm (MIPSO), a modified version of Particle Swarm Optimization, is integrated with the GRIDMAP framework to improve solution accuracy by factoring in both installation and customer interruption costs within the grid model. Additionally, GRIDMAP streamlines interruption duration calculation by efficiently analyzing both temporary and permanent faults through matrix-based comparisons of fault locations, load points, and protective devices. This built-in logic enables rapid, automated calculation of interruption durations, enhancing the accuracy and practicality of reliability assessments.

The remainder of the paper is structured as follows. Section 2 describes the problem formulation. Section 3 presents the model, including the objective function and constraints. Case studies and results are discussed in Section 4, followed by conclusions in Section 5.

2. Problem Description

In the field of power distribution grids, the reliability and efficiency of grid operations are significantly influenced by the strategic placement of protective and control devices, such as Re, Sec, Fu, RCS, and Ms. These devices are essential for safeguarding the grid against faults and ensuring quick service restoration. However, the lack of a comprehensive and effective modeling approach has made the optimal allocation of these devices a complex challenge. Existing methods often fail to accurately capture the intricate interactions between grid components, fault probabilities, and geographical layouts, leading to suboptimal device placement decisions. The absence of a suitable modeling framework for distribution grids has limited the ability to assess the grid's behavior in various fault scenarios, resulting in increased system downtime, higher maintenance costs, and reduced reliability. This gap in the existing methodologies highlights the need for a

more systematic and scalable model. In response, this study proposes a novel approach through GRIDMAP, which offers a more precise and effective way of representing complex distribution grid topologies. The GRIDMAP model not only addresses the existing limitations but also provides a robust foundation for optimal device placement. By incorporating this model, the study optimizes the allocation of protective and control devices with the goal of minimizing interruption durations and improving overall grid reliability. Furthermore, this approach can be extended to broader distribution grid analysis and planning, making it a versatile tool for grid management. Figure 1 illustrates how the proposed GRIDMAP model addresses challenges in conventional planning methods.

Figure 1: Challenges Overcome by the Proposed GRIDMAP Model

3. Methodology

3.1. Introduction to the GRIDMAP Framework

The GRIDMAP matrix structure is mathematically justified through a structured mapping of the distribution network, modeled as a directed acyclic graph (DAG) $G = (V, E)$, where V represents the set of nodes (e.g., buses, nodes) and $E \subseteq (V \times V)$ denotes the set of directed edges (feeder sections). To systematically encode this topology, GRIDMAP introduces a matrix $M \in \mathbb{R} \rightarrow n \times (m + 1)$, where n denotes the maximum number of nodes along the main feeder (i.e., the depth of the feeder tree), and m represents the maximum number of nodes in any branch feeder. Each node $v \in V$ is uniquely mapped to a matrix position $f(v) = (i, j)$, with row index i indicating the vertical (depth) position within a feeder path, and column index j identifying the specific branch or sub-branch to which the node belongs. This injective mapping ensures a lossless representation, preserving both the identity and relative topological positioning of each node in the network. The hierarchical relationship is preserved by interpreting nodes with higher row indices as downstream, and, when row indices are equal, nodes with higher column indices as further downstream in the same hierarchical level. As such, unlike a standard adjacency matrix, which merely represents the existence of connections

between nodes in a graph, the GRIDMAP matrices provide a richer representation of power distribution systems by incorporating topological structure, operational data, and device placement information. This distinction is clearly outlined in Table 2, which compares the two approaches in terms of structure, purpose, and application.

Table 2: Comparison Between Adjacency Matrix and GRIDMAP Matrices

To facilitate comprehensive analysis and planning in distribution grids, this study introduces GRIDMAP, a structured framework that models the topology of power distribution systems using graph and matrix representations. Within this framework, the distribution grid is represented as a directed graph, where nodes correspond to key components such as transformers, feeder sections, and protective devices and edges denote the physical and operational interconnections between these elements. Each node is associated with a set of attributes, including load characteristics and protection device types. GRIDMAP leverages this graph structure to support detailed analysis of grid behavior under a variety of fault scenarios, enabling targeted strategies for fault detection, isolation, and service restoration. A central feature of GRIDMAP is its matrix-based data architecture, which organizes grid topology into structured matrices. In this formulation, n denotes the maximum number of buses on the main feeder, while m represents the maximum number of buses within the largest branch feeder. The resulting matrices possess dimensions of $n \times (m + 1)$, with the exception of matrix x , which is defined as $n \times 2$ to reflect two candidate installation points per feeder section. The additional column $(m + 1)$ ensures the representation of the main feeder in the first row, followed sequentially by data for each branch feeder, ordered from upstream to downstream. Matrices (1), (2), and (3) specifically represent the candidate installation points, grid loads, and feeder section information, respectively. Notably, the final three rows in the load and feeder matrices are zero-filled, indicating that the corresponding nodes (nodes 2 through 4) do not possess downstream branches or sub-branches.

The initialization and interpretation of these matrices become more intuitive when compared with the grid diagram illustrated in Figure 2, as the spatial layout and matrix positions are directly aligned. This structural

alignment enhances both interpretability and computational efficiency during grid status evaluations. A key analytical capability of the GRIDMAP framework lies in its support for hierarchical load and feeder section comparison. When comparing matrix elements, the row indices are first assessed higher row numbers indicate downstream positioning. If row indices are equal, column indices are compared, with the larger index also indicating a downstream location. For example, if feeder section b appears in the first row of the feeder matrix and load l_{m2} in the second row of the load matrix, l_{m2} is considered downstream of section b . In contrast, if both a feeder section and a load reside in the same row but occupy different columns, the one with the smaller column number is deemed upstream. Through this systematic modeling strategy, GRIDMAP ensures consistent and reliable topological comparisons. It also supports robust analysis of load interruptions. Moreover, it offers a scalable foundation for future improvements in distribution system monitoring, control, and planning. The following sections present the mathematical formulation for the optimal placement of protection and control devices within the distribution grid. Based on the GRIDMAP framework, this problem can be modeled in a way that accounts for the complex topology of large-scale distribution grids. The objective function and the corresponding constraints for the problem will be defined, highlighting the significance of the proposed matrix-based structure in efficiently solving the problem for large and intricate grids. In this context, it is important to note that the index i refers to the row indices of the matrices, while ii denotes the column indices. These notations will play a crucial role in formulating the relationships and constraints that define the optimal placement problem. With the integration of this model, a scalable and flexible approach is introduced for addressing complex distribution grid configurations, facilitating more effective planning and decision-making for grid operators.

Figure 2: Sample distribution grid model

$$X = \begin{bmatrix} x_{1,1} & x_{1,2} & x_{1,3} & x_{1,4} & x_{1,5} & x_{1,6} & x_{1,7} & x_{1,8} \\ x_{2,1} & x_{2,2} & x_{2,3} & x_{2,4} & x_{2,5} & x_{2,6} & 0 & 0 \\ x_{3,1} & 0 & 0 & 0 & 0 & 0 & 0 & 0 \\ x_{4,1} & 0 & 0 & 0 & 0 & 0 & 0 & 0 \\ x_{5,1} & 0 & 0 & 0 & 0 & 0 & 0 & 0 \end{bmatrix} \quad (1)$$

$$load = \begin{bmatrix} 0 & l_{n2} & l_{n3} & l_{n4} \\ l_{m1} & l_{m2} & l_{m3} & 0 \\ 0 & 0 & 0 & 0 \\ 0 & 0 & 0 & 0 \\ 0 & 0 & 0 & 0 \end{bmatrix} \quad (2)$$

$$Feeder\ section = \begin{bmatrix} a & b & c & d \\ e & f & g & 0 \\ 0 & 0 & 0 & 0 \\ 0 & 0 & 0 & 0 \\ 0 & 0 & 0 & 0 \end{bmatrix} \quad (3)$$

3.2. Objective Function and Parameters

The primary objective of this research is to minimize the total interruption duration across the power distribution grid. To achieve this, an objective function is defined, which incorporates various parameters, including the reliability indices of the protective devices, the load demand at different nodes, and the fault probabilities associated with each segment of the grid. The objective function can be mathematically expressed as follows Eq.4:

$$Minimize[C^{eq} + C^{du}] \quad (4)$$

In Equation (1), C^{eq} denotes the costs associated with the devices, whereas C^{du} represents the costs incurred by customers due to interruptions in the distribution grid. equation Eq.5 reflects the cost of the devices utilized in the grid. Therefore, the overall cost of the devices can be represented as:

$$C^{eq} = C^{PS} + C^{CS} \quad (5)$$

C^{PS} represents the cost of protective devices, while C^{CS} refers to the cost of control devices. equation Eq.6 covers the initial investment in the first year, along with the maintenance costs of the protective devices, which are denoted as C^{PS} in equation Eq.5. Similarly, equation Eq.7 applies to control devices, represented as C^{CS} in equation Eq.5.

$$\begin{aligned}
C^{PS} = & \sum_{(i=1)}^n \sum_{(ii=1)}^m ((IC_{(i,ii)}^{Re} \cdot IX_{(i,ii)}^{Re}) + (IC_{(i,ii)}^{fu} \cdot IX_{(i,ii)}^{fu})) \\
& + \sum_{(i=1)}^n \sum_{(ii=1)}^m ((RC_{(i,ii)}^{Re} \cdot RX_{(i,ii)}^{Re}) + (RC_{(i,ii)}^{fu} \cdot RX_{(i,ii)}^{fu})) \\
& + \sum_{(i=1)}^t \sum_{(j=1)}^n \sum_{(jj=1)}^m \left(\frac{1+\alpha}{1+d}\right)^i \cdot ((MC_{(j,jj)}^{Re} \cdot MX_{(j,jj)}^{Re}) + (MC_{(j,jj)}^{fu} \cdot MX_{(j,jj)}^{fu}))
\end{aligned} \tag{6}$$

$$\begin{aligned}
C^{CS} = & \sum_{(i=1)}^n \sum_{(ii=1)}^m ((IC_{(i,ii)}^{sec} \cdot IX_{(i,ii)}^{sec}) + (IC_{(i,ii)}^{RCS} \cdot IX_{(i,ii)}^{RCS}) + (IC_{(i,ii)}^{MS} \cdot IX_{(i,ii)}^{MS})) \\
& + \sum_{(i=1)}^n \sum_{(ii=1)}^m ((RC_{(i,ii)}^{sec} \cdot RX_{(i,ii)}^{sec}) + (RC_{(i,ii)}^{RCS} \cdot RX_{(i,ii)}^{RCS}) + (RC_{(i,ii)}^{MS} \cdot RX_{(i,ii)}^{MS})) \\
& + \sum_{(i=1)}^t \sum_{(j=1)}^n \sum_{(jj=1)}^m \left(\frac{1+\alpha}{1+d}\right)^i \cdot ((MC_{(j,jj)}^{sec} \cdot MX_{(j,jj)}^{sec}) + (MC_{(j,jj)}^{RCS} \cdot MX_{(j,jj)}^{RCS}) + (MC_{(j,jj)}^{MS} \cdot MX_{(j,jj)}^{MS}))
\end{aligned} \tag{7}$$

In Eq.6, the following symbols are defined: $IC_{(i,ii)}^{(Re/fu)}$ represents the initial purchase cost of Re/Fu, $RC_{(i,ii)}^{(Re/fu)}$ represents the relocation costs of the devices, which varies as a three-dimensional matrix for each candidate location in the grid. $X_{(i,ii)}^{(Re/fu)}$ refers to the coordinates of the candidate points for device installation, indicating which device is installed at which candidate location. $IX_{(i,ii)}^{(Re/fu)}$ Refers to which switch should be purchased for which coordinates. $RX_{(i,ii)}^{(Re/fu)}$ refers to the coordinates of the candidate points where devices have been relocated for installation. If a device is already present in the circuit but is not in the correct location, this value will be set to one to facilitate the calculation of the relocation cost. The term $\left(\frac{1+\alpha}{1+d}\right)^i$ is the conversion factor used to adjust future costs to present value, considering the inflation rate α and the interest rate d . Additionally, $MC_{(j,jj)}^{(Re/fu)}$ represents the annual maintenance costs of protective devices, which also vary by candidate location, similar to the initial purchase costs. The symbols in equation Eq.7 are similar to those in equation Eq.6. interruption Costs represent the financial losses of customers due to service disruptions caused by device failures or grid faults. equation Eq.8 calculates the interruption costs of the grid.

$$C^{du} = C^P + C^T \tag{8}$$

In equation Eq.8, C^P and C^T represent the interruption costs from permanent and temporary failures, respectively. equation Eq.9 quantifies the costs from permanent failures, while equation Eq.10 calculates the costs from temporary failures.

$$C^P = \sum_{(i=1)}^t \sum_{(i=1)}^n \sum_{(ii=1)}^m \sum_{(j=1)}^n \sum_{(jj=1)}^m \left(\left(\frac{1+\alpha}{1+d} \right)^i \cdot (\lambda_{(i,ii)}^P \cdot (load_{(j,jj,k)} \cdot (1+Lr)^i) \cdot cdf_{(j,jj,k)} \cdot dr_{(j,jj)}^T) \right) \quad (9)$$

$$C^T = \sum_{(i=1)}^t \sum_{(i=1)}^n \sum_{(ii=1)}^m \sum_{(j=1)}^n \sum_{(jj=1)}^m \left(\left(\frac{1+\alpha}{1+d} \right)^i \cdot (\lambda_{(i,ii)}^T \cdot (load_{(j,jj,k)} \cdot (1+Lr)^i) \cdot cdf_{(j,jj,k)} \cdot dr_{(j,jj)}^T) \right) \quad (10)$$

In equations Eq.9 and Eq.10, $\lambda_{(i,ii)}^{(P/T)}$ represents the annual failure rates for permanent and temporary interruptions, varying across grid points. Lr annual electricity load growth rate, $load_{(j,jj,k)}$ is the average demand load, and (k) denotes the consumer type, $dr_{(j,jj)}^{(P/T)}$ indicates the interruption duration, while $cdf_{(j,jj,k)}$ is the cost function for customer losses, depending on the consumer type. Three consumer types are considered: residential, commercial, and industrial. The problem's constraints and objective function specifications are provided below.

3.3. Stability and Superiority of the Modified PSO Algorithm Combined with GRIDMAP

To evaluate the performance of metaheuristic algorithms in solving complex optimization problems, three widely used methods Modified Particle Swarm Optimization (MIPSO), Imperialist Competitive Algorithm (ICA), and Ant Colony Optimization (ACO) were compared in terms of both algorithmic characteristics and numerical results. A summary of each algorithm's conceptual foundation is provided in Table 3. MIPSO, inspired by the collective behavior of birds and fish, benefits from a high convergence speed and simple implementation. In contrast, ICA simulates socio-political competition among empires, while ACO is based on the pheromone-based pathfinding behavior of ants. In terms of general characteristics, MIPSO shows clear advantages over ACO and ICA. As illustrated in Table 4, it offers high convergence speed, simple implementation, and applicability to both discrete (with modifications) and continuous problems, making it a versatile and efficient option.

Table 3: Metaheuristic Algorithms and Their Inspirations

Table 4: General Characteristics of Algorithms

3.3. Constraints and modifications of the Algorithm

In the standard PSO (Particle Swarm Optimization) algorithm, decision variables are typically continuous. However, in this problem, the decision variables are discrete integers ranging from 0 to 5. To address this, a rounding process is applied to convert continuous variables into integers. These integer values are then transformed into a matrix of candidate point variables, as shown in Matrix (1). This adaptation is illustrated in Figure 3, where the PSO algorithm is modified to the MIPSO (Modified PSO) algorithm. The transformation process is depicted in Figure 4. Initially, the PSO algorithm generates continuous decision variables between 0 and 5, representing potential device placements. A rounding process is then applied to convert these into discrete integer values. Based on these integers, five binary chromosomes are generated, each corresponding to a specific type of device. A value of 0 indicates no device, while values 1 to 5 represent distinct devices: 1 for Re, 2 for Fu, 3 for Sec, 4 for RCS, and 5 for Ms. This two-step transformation allows the PSO algorithm to handle discrete decision-making, ensuring each candidate location receives exactly one device while adhering to the problem's constraints. If a device is already placed at a location, it is checked for correctness; if necessary, it is repositioned.

Figure 3: The MIPSO Algorithm

Figure 4: Binary encoding process

3.4. Placement and Relocation in GRIDMAP

The implementation of equipment placement and relocation within the GRIDMAP model is straightforward and highlights the method's flexibility. The decision-making process, as shown in Figure 5, involves the evaluation of each candidate point to determine the appropriate action. This efficient process, clearly depicted in the flowchart, is seamlessly incorporated into the GRIDMAP model. The ability to handle equipment relocation and installation with ease demonstrates the flexibility and adaptability of the model in real-world scenarios, making it a powerful tool for optimizing equipment placement in complex distribution

grids. Overall, the GRIDMAP model offers a comprehensive, adaptable, and efficient solution for optimizing equipment placement, ensuring reliable and cost-effective grid operations in dynamic environments.

Figure 5: Decision-Making Process for Candidate Point Evaluation

3.5. Fault-Driven Interruption Analysis in GRIDMAP

Accurately calculating interruption durations is essential for evaluating the performance of protective devices and the overall reliability of the distribution grid. In this study, the fault model simplifies faults into two main categories: permanent and temporary. This approach is consistent with widely accepted practices, including the IEEE 1366 standard, which emphasizes these categories for reliability and interruption analysis. Although complex faults such as multiple simultaneous faults caused by lightning strikes are acknowledged, incorporating correlation models for such faults is beyond the scope of this work. The simplification allows for a clearer and more focused evaluation of interruption durations, maintaining a balance between model accuracy and analytical tractability. The GRIDMAP model provides a structured and flexible framework for this purpose by leveraging matrix-based representations of the grid. The fault locations are specified through coordinate values in the matrices, which define their positions along the feeder sections. These coordinates are then compared against the grid's load matrix to determine which loads are affected. For instance, as illustrated in Figure 6, if a permanent fault occurs in feeder section d, its coordinates are recorded in Matrix (3).

Figure 6: Interruption Duration Calculation for Temporary and Permanent Faults in Power Grids

To evaluate the resulting impact, this matrix is compared with Matrix (2), which contains the coordinates of all loads. Additionally, by referencing Matrix (1) which holds the locations and types of installed devices the model determines whether a protective device isolates the fault or allows the interruption to propagate downstream. This systematic comparison identifies the exact loads affected by a given fault. In the case of the fault in section d, only load L_{n4} is disconnected and remains out of service until the fault is resolved. This precise tracking of interruption effects is seamlessly integrated into the GRIDMAP structure, demonstrating the model's strength in handling both fault localization and interruption analysis. The specific steps involved

in calculating interruption durations for permanent faults are explained in detail in Section B of Figure 6. For temporary faults, which are typically transient in nature, the algorithm simulates the automatic restoration capabilities of devices such as reclosers (Re). The duration of temporary faults is generally shorter and is calculated as shown in Section A of Figure 6. By analyzing each fault type separately, this approach enables precise evaluation of grid reliability and device allocation impact, supporting better real-world decision-making.

4. Numerical results

4.1 Test System and Assumptions

The Figure 7 illustrates the modified IEEE 69-bus standard distribution system, employed in this study as a representative real-world grid with multiple branched configurations. This grid serves as a practical testbed for evaluating the performance of the proposed algorithm and conducting comprehensive sensitivity analyses. The use of this system highlights the flexibility and capability of the GRIDMAP modeling framework in accurately representing complex and branched distribution grids. Through this model, it becomes feasible to simulate realistic operational scenarios and investigate the optimal allocation of protection and control devices under diverse conditions, reflecting the practical challenges encountered in modern power distribution systems. In Table 5, the grid's information and parameters are assumed to approximate the ideal real-world conditions. Additionally, the temporary failure rate in the feeders is assumed to be four times the permanent failure rate. This study evaluates the capital investment costs for key components, including the recloser, Sec, RCS, and MS, along with relocation and maintenance expenses. Customer Damage Functions (CDFs) for various interruption durations are adopted from [1]. The planning horizon spans 15 years, with an annual load growth rate of 3% and an interest rate of 8%. Repair parameters include 5 minutes for remote switching, 60 minutes for manual switching, and 180 minutes for fault repair. The Sec operates automatically within 1 second, while loads protected by the downstream recloser experience no interruptions. The proposed model was implemented in the MATLAB R2015 environment.

The developed model was executed using a laptop equipped with an Intel Pentium® CPU N4200 running at 1.1 GHz and 8 GB of RAM. All case studies were solved in less than 30 minutes, demonstrating the efficiency of the solver.

Table 5: Parameters of IEEE 69 Bus System

Figure 7: The modified IEEE 69-bus system

4. 2 Results and Discussion

In this study, the MIPOS algorithm was evaluated through four distinct scenarios applied to the modified IEEE 69-bus system standard distribution grid. The scenarios were designed to examine the impact of optimal device allocation on the reliability and efficiency of the system.

Scenario 1: optimal allocation without existing equipment, focused on determining the optimal allocation of protection devices without considering the existing equipment already installed in the grid. This approach provides a baseline for assessing the potential improvements in reliability when no initial equipment are installed.

Scenario 2: optimal allocation considering existing equipment, the existing devices listed in Table 6 were considered as part of the initial setup. This scenario allows for a more realistic evaluation of the optimal allocation of new devices, taking into account the already installed protection devices in the grid.

Table 6: Location of Primary Devices

Scenario 3: allocation of devices at branch starting points, aimed to analyze the effect of placing devices exclusively at the beginning of each feeder section. This scenario is designed to test the hypothesis that allocation at the beginning of the branch could improve the overall grid reliability by minimizing the impact of faults and reducing the restoration time. Scenario 4: allocation of devices at branch endpoints, explored the opposite approach, where devices were placed only at the endpoints of the feeder sections. This scenario was crucial for evaluating the performance of devices placed at the extremities of the grid, where fault isolation and restoration are often more challenging. Tables 7–10 provide a detailed overview of the selected

device types, numbers, and locations for each of the scenarios mentioned above. The results obtained from these scenarios are summarized in Table 11 for comparison, and will be further discussed in the following, with an emphasis on how different allocation strategies impact system reliability, fault detection, and restoration time.

Table 7: Devices Placed (Scenario 1)

Table 8: Devices Placed (Scenario 2)

Table 9: Devices Placed (Scenario 3)

Table 10: Devices Placed (Scenario 4)

Table 11: Comparison of Scenarios

Scenario 1 shows the highest total cost of \$628,270. The major contributing factor to this high cost is the significant customer interruption cost (C^P), which represents a high impact of permanent faults. The equipment cost is also notable, as no existing equipment is considered in this scenario, resulting in higher initial investment in protective devices. The time to solve (1,452 seconds) is the longest among the scenarios, indicating a more complex optimization problem. Overall, this scenario provides a comprehensive but costlier strategy for fault isolation.

Scenario 2 shows a reduction in total cost by 2.93% compared to Scenario 1. The main reduction comes from a lower equipment cost due to the inclusion of existing devices, which reduces the need for new installations. The customer interruption cost (C^P) decreases slightly to \$507,980, which still represents a significant amount, but the cost of temporary interruptions (C^T) is also reduced by 5.33% to \$1,084. The time to solve also decreases by 14.2% (206 seconds), showing a more efficient optimization process when existing equipment is taken into account. This scenario better succeeds in making a balance between cost and reliability. Scenario 3, focusing on the allocation of devices at the beginning of feeder sections, has the lowest total cost, showing a 3.64% decrease compared to Scenario 2. The customer interruption cost (C^P) is reduced to \$497,390, equivalent to a 2.1% decrease, while the temporary interruption cost (C^T) also

significantly drops by 41.89%. The equipment cost is lower, indicating that fewer devices are needed. The time to solve increases slightly (by 3.12%, or 39 seconds), likely due to the more focused optimization on specific locations (branch start points). This scenario provides a cost-effective solution with efficient fault isolation at branch start points. Scenario 4 shows the highest total cost, which is a 14.71% increase compared to Scenario 3. The main factor contributing to this increase is the high customer interruption cost (C^P), reflecting the inefficiency of placing devices only at the ends of branches. While the device cost (\$80,461) is the lowest, it cannot compensate for the higher interruption costs. The temporary interruption cost (C^T) remains relatively unchanged. The time to solve is the shortest at 1,098 seconds, suggesting a less complex optimization process compared to other scenarios, but the allocation strategy itself results in a less effective grid performance.

Scenario 3 is the most cost-effective, with a total cost of \$587,580, which is 6.96% lower than Scenario 1. This is due to the optimized device allocation at branch start points, which leads to a lower customer interruption cost (C^P) and a significant reduction in temporary interruption costs (C^T). The overall device cost is also lower compared to the other scenarios, making it the most efficient configuration in terms of both cost and reliability. Comparing Scenario 1 and Scenario 2 shows that including existing equipment leads to a reduction in device costs by approximately 15.2%. However, the customer interruption cost (C^P) remains high, reflecting that despite the reduced equipment cost, the effectiveness of the protection strategy is not significantly improved. The slight reduction in total cost (2.93%) suggests that while using existing equipment helps in reducing the capital expenditure, it does not drastically change the grid's reliability in case of faults.

Scenario 4, which places devices only at the end of branches, results in the highest total cost due to the inefficient allocation strategy. The customer interruption cost (C^P) increases by 21.6% compared to Scenario 3, indicating that placing devices at the end of branches may not be an optimal solution for fault isolation and minimizing the impact of faults. This shows that the allocation of devices at the beginning of

branches (as seen in Scenario 3) is a more reliable and cost-effective strategy. The time to solve the optimization problem decreases as we move from Scenario 1 to Scenario 4. This indicates that the problem becomes less complex when more constraints are imposed (i.e., when existing equipment is considered, or when device allocation is restricted to certain points like branch ends). Scenario 4, with the smallest search space, has the shortest time to solve at 1,098 seconds.

4.3. Analysis of Numerical Results and Algorithm Performance

The numerical results from single-run experiments are summarized in Table 12. MIPSO achieved the lowest total cost (\$628,270) and the shortest solving time (1,452 seconds) compared to ACO and ICA. These results indicate a significant improvement in both solution quality and computational efficiency when MIPSO is used in combination with the GRIDMAP modeling framework, which enables detailed spatial and structural modeling of the problem domain. To further validate the stability and robustness of MIPSO, the algorithm was executed ten consecutive times in combination with GRIDMAP. The results, shown in Table 13, reveal minimal variations in total cost and solution time. The total cost remained within a narrow range (\$617,000 to \$628,700), demonstrating consistent convergence behavior and reliable performance across different runs.

Table 12: Performance Comparison of Algorithms (Single Run)

Table 13: Stability Analysis of MIPSO + GRIDMAP (10 Runs)

Based on both comparative characteristics (Table 3 and 4) and numerical results (Tables 12 and 13), the Modified PSO algorithm, especially when combined with the GRIDMAP framework, demonstrates clear advantages over ICA and ACO. It not only produces more cost-effective and time-efficient solutions but also ensures high stability across multiple executions. These qualities make MIPSO a highly reliable and scalable metaheuristic approach for solving complex, real-world optimization problems.

4.4. Sensitivity analysis

The rate of electrical load growth significantly impacts the performance and stability of distribution grids. As demand increases, it can strain infrastructure, leading to overloads, inefficiencies, and more faults.

Managing this growth is crucial for reliable operation. This section explores the effects of varying load growth rates on the grid, particularly focusing on the role of protection and control devices (e.g., Re, sec, switches) in fault isolation and system recovery. A stepwise approach was used to analyze the grid's sensitivity to load growth, with results shown in Table 14 and Figure 8 illustrating the number of devices needed as load growth increases.

Table 14: the effects of increasing rates (Lr)

Figure 8: Protective and control device quantity

Impact on Total Cost: As the annual load growth rate (Lr) increases, the total cost steadily rises. For instance, when Lr increases from 0.03 to 0.12, the total cost rises from \$628,270 to \$1,097,000, marking an increase of 74.8%. This increase is primarily due to the higher stress placed on the system, which necessitates the installation of more equipment and more complex protection strategies to handle the growing demand. The customer interruption cost (C^P) follows a similar trend, increasing as Lr grows. From \$508,370 at $Lr = 0.03$, it rises to \$868,520 at $Lr = 0.12$ (a 70.9% increase). This suggests that as the load increases, the grid is more susceptible to permanent faults, requiring more effective fault isolation and restoration strategies to minimize customer interruption impacts. Temporary interruption costs (C^T) also increase with the load growth rate, though the rate of increase is less pronounced than that of permanent interruptions. For example, (C^T) rises from \$1,145 at $Lr = 0.03$ to \$1,984 at $Lr = 0.12$, indicating that with higher load growth, the frequency and severity of temporary interruptions also increase. The cost of protective devices increases significantly as the load growth rate rises. It goes from \$118,760 at $Lr = 0.03$ to \$226,510 at $Lr = 0.12$, an increase of 90.6%. This is due to the need for additional protective and control devices (e.g., Re, Sec, Fu, and switches) to cope with the rising load and ensure system reliability under higher demand conditions. The time to solve the optimization problem shows minor fluctuations in response to changes in the load growth rate. From 1,452 seconds at $Lr = 0.03$, it decreases slightly to 1,439 seconds at $Lr = 0.06$, indicating a slightly more efficient optimization process. However, the time remains relatively consistent across the different

growth rates, suggesting that the primary challenge lies in the physical and operational changes required in the grid, rather than in computational complexity. The number of devices required for the grid also increases as the load growth rate rises. Particularly, the number of Re, Fu, RCS, and MS all increase with higher load growth rates. This highlights the need for more comprehensive protection and control measures as the system adapts to higher electricity demand.

4.4.1. Considering Equipment Heterogeneity

In real-world systems, equipment differs by quality, price, and reliability, which affects both purchase and maintenance costs as well as failure rates. To analyze the impact of this heterogeneity, three scenarios were developed:

- Scenario 1: A single equipment type with purchase and maintenance costs (base case).
- Scenario 2: Two equipment types; the second type costs 10% more but has a 30% lower maintenance cost.
- Scenario 3: Three equipment types; each subsequent type costs 10% more than the previous one (i.e., type 2 is 10% and type 3 is 20% more expensive than the base), with maintenance costs reduced by 30% and 50%, respectively.

Table 15 compares the outcomes of the three scenarios with different levels of equipment heterogeneity.

Table 15: Impact of Equipment Heterogeneity on Total Cost and Computational Performance

Increasing equipment heterogeneity leads to a slight rise in the total system cost, mainly due to the higher purchase prices of higher-quality equipment. In Scenarios 2 and 3, the costs of both temporary and permanent outages also show a slight increase. Due to the high cost of the equipment, a smaller number of units were likely selected. This limitation significantly reduced overall system coverage and consequently failed to adequately prevent failures and downtimes. Additionally, solution time increases significantly due to the greater model complexity introduced by a broader set of equipment options, which expands the search space

and raises the risk of convergence to local optima. Therefore, although higher-quality equipment may reduce maintenance needs, the associated increase in purchase costs and decision-making complexity ultimately leads to higher total costs and longer computation times. These findings highlight the need for careful consideration when incorporating equipment heterogeneity, ensuring a balanced trade-off between technical benefits, economic costs, and computational feasibility.

5. Conclusion

This study introduced an advanced modeling and optimization framework for the optimal allocation of protection and control devices Re, Fu, Sec, RCS, and MS in power distribution systems. At the core of this approach lies the GRIDMAP modeling structure, which enables a detailed and flexible representation of real-world, large-scale, and branched distribution grids. This structured modeling not only facilitates accurate fault localization and load tracking but also seamlessly integrates with the proposed Modified Integer PSO (MIPSO) algorithm for efficient decision-making. By embedding installation, interruption, and relocation costs within the optimization process, the proposed method provides a realistic and practical solution that considers existing equipment and their potential repositioning. The proposed MIPSO model, compared to ACO and ICA, achieved the lowest total cost and fastest computation time in single-run experiments. Stability was confirmed over 10 runs, showing minimal variation in results. Sensitivity analysis on equipment heterogeneity revealed that while higher-quality equipment reduces maintenance costs, it increases total cost and computation time due to added model complexity. The results from the four evaluated scenarios underline the significance of both accurate modeling and strategic device placement. Scenario 3, which leverages the model's structure to place devices near branch origins, delivered the most reliable and cost-effective outcome. In contrast, Scenario 4, with devices placed at endpoints, proved less efficient highlighting the impact of topology-aware modeling in optimizing grid performance. Furthermore, the sensitivity analysis demonstrated that demand growth directly affects both interruption costs and device requirements, emphasizing the necessity for proactive grid planning that anticipates future grid demands.

The ability of GRIDMAP to model and adapt to such changes in grid conditions further proves its flexibility and power in representing real-world distribution grid challenges. In conclusion, the study emphasizes the importance of integrating intelligent device placement with realistic, real-world constraints such as existing equipment, relocation possibilities, and future load growth. The proposed method offers several key advantages, most notably the GRIDMAP framework's structured matrix representation, which enables high scalability and seamless compatibility with various optimization techniques, including metaheuristic algorithms. Additionally, the built-in mechanism for identifying and relocating existing devices enhances economic efficiency by reducing redundant installations. However, the method also presents certain limitations. The reliance on matrix-based models and advanced optimization algorithms such as MIPSO may lead to increased computational complexity and require substantial processing resources, particularly in large-scale networks. Furthermore, the model's effectiveness depends on the availability of accurate and comprehensive data related to network topology, equipment locations, and load characteristics data which may be incomplete or inconsistent in real-world scenarios. Lastly, the implementation of GRIDMAP and MIPSO can be technically demanding, posing challenges for engineers unfamiliar with such advanced modeling and optimization frameworks. In any case, it not only offers a solid foundation for real-world applications but also provides a stepping stone for future research in adaptive, AI-driven grid planning and optimization in large-scale, complex grids.

Acknowledgements

The corresponding author wishes to acknowledge the financial support provided by the Research Council of Shahid Chamran University of Ahvaz, Iran (Grant no. SCU.EE1403.37219).

References

- [1] Azarhazin S., Farzin H., and Mashhour E., "An MILP model for reliability-based placement of recloser, sectionalizer, and disconnect switch considering device relocation," *Sustainable Energy, Grids and Networks*, vol. 35, p. 101127, 2023. DOI: <https://doi.org/10.1016/j.segan.2023.101127>
- [2] Usama, M., Mokhlis, H., Moghavvemi, M., Mansor, N.N., Alotaibi, M.A., Muhammad, M.A. and Bajwa, A.A., "A comprehensive review on protection strategies to mitigate the impact of renewable energy sources on interconnected distribution networks," *IEEE Access*, vol. 9, pp. 35740-35765, 2021. DOI: <https://doi.org/10.1109/access.2021.3061919>

- [3] Chandra A., Singh G. K., and Pant V., "Protection of AC microgrid integrated with renewable energy sources—A research review and future trends," *Electric Power Systems Research*, vol. 193, p. 107036, 2021. DOI: <https://doi.org/10.1016/j.epsr.2021.107036>
- [4] Al Hadi A., Silva C. A. S., Hossain E., and Chaloo R., "Algorithm for demand response to maximize the penetration of renewable energy," *IEEE Access*, vol. 8, pp. 55279-55288, 2020. DOI: <https://doi.org/10.1109/access.2020.2981877>
- [5] El-maksoud A., Ahmed A., and Hasan S., "Simultaneous Optimal Network Reconfiguration and Allocation of Four Different Distributed Generation Types in Radial Distribution Networks Using a Graph Theory-Based MPSO Algorithm," *International Journal of Intelligent Engineering & Systems*, vol. 16, no. 2, 2023. DOI: <https://doi.org/10.22266/ijies2023.0430.24>
- [6] Hamidan M.-A. and Borousan F., "Optimal planning of distributed generation and battery energy storage systems simultaneously in distribution networks for loss reduction and reliability improvement," *Journal of Energy Storage*, vol. 46, p. 103844, 2022. DOI: <https://doi.org/10.1016/j.est.2021.103844>
- [7] Kim R.-K., Glick M. B., Olson K. R., and Kim Y.-S., "MILP-PSO combined optimization algorithm for an islanded microgrid scheduling with detailed battery ESS efficiency model and policy considerations," *Energies*, vol. 13, no. 8, p. 1898, 2020. DOI: <https://doi.org/10.3390/en13081898>
- [8] Aldhubaib H. A., Ahmed M. H., and Salama M. M., "A weather-based power distribution system reliability assessment," *Alexandria Engineering Journal*, vol. 78, pp. 256-264, 2023. DOI: <https://doi.org/10.1016/j.aej.2023.07.033>
- [9] Blinov I., Zaitsev I., Parus E., and Bereznychenko V., "Faults Indicators applying for smart monitoring system for improving reliability electric power distribution," in *Power Systems Research and Operation: Selected Problems II*: Springer, 2022, pp. 235-256. DOI: https://doi.org/10.1007/978-3-031-17554-1_11
- [10] Meera P. and Hemamalini S., "Reliability assessment and enhancement of distribution networks integrated with renewable distributed generators: A review," *Sustainable Energy Technologies and Assessments*, vol. 54, p. 102812, 2022. DOI: <https://doi.org/10.1016/j.seta.2022.102812>
- [11] Ghosh P. and De M., "A comprehensive survey of distribution system resilience to extreme weather events: concept, assessment, and enhancement strategies," *International Journal of Ambient Energy*, vol. 43, no. 1, pp. 6671-6693, 2022. DOI: <https://doi.org/10.1080/01430750.2022.2037460>
- [12] Hasankhani A. and Hakimi S. M., "Stochastic energy management of smart microgrid with intermittent renewable energy resources in electricity market," *Energy*, vol. 219, p. 119668, 2021. DOI: <https://doi.org/10.1016/j.energy.2020.119668>
- [13] Borowski P. F., "Zonal and Nodal Models of energy market in European Union," *Energies*, vol. 13, no. 16, p. 4182, 2020. DOI: <https://doi.org/10.3390/en13164182>
- [14] Dwivedi, D., Mitikiri, S.B., Babu, K.V.S.M., Yemula, P.K., Srinivas, V.L., Chakraborty, P. and Pal, M., "Technological advancements and innovations in enhancing resilience of electrical distribution systems," *International Journal of Critical Infrastructure Protection*, p. 100696, 2024. DOI: <https://doi.org/10.1016/j.ijcip.2024.100696>
- [15] Mahdavi M., Alhelou H. H., Gopi P., and Hosseinzadeh N., "Importance of radiality constraints formulation in reconfiguration problems," *IEEE Systems Journal*, vol. 17, no. 4, pp. 6710-6723, 2023. DOI: <https://doi.org/10.1109/jsyst.2023.3283970>
- [16] Mahdavi M., Schmitt K., Jurado F., Awaaf A., and Chamana M., "An efficient framework for optimal allocation of renewable energy sources in reconfigurable distribution systems with variable loads," *IEEE Transactions on Industry Applications*, vol. 60, no. 2, pp. 2431-2442, 2023. DOI: <https://doi.org/10.1109/tia.2023.3341876>
- [17] Mahdavi M., Schmitt K., Chamana M., and Bayne S., "Distribution systems reconfiguration considering dependency of loads on grid voltage and temperature," *IEEE Transactions on Power Delivery*, vol. 39, no. 2, pp. 882-897, 2023. DOI: <https://doi.org/10.1109/tpwr.2023.3340344>
- [18] Meng, X., Sun, C., Mei, J., Tang, X., Hasanien, H.M., Jiang, J., Fan, F. and Song, K., "Fuel cell life prediction considering the recovery phenomenon of reversible voltage loss," *Journal of Power Sources*, vol. 625, p. 235634, 2025. DOI: <https://doi.org/10.1016/j.jpowsour.2024.235634>
- [19] Tang X., Shi L., Li M., Xu S., and Sun C., "Health state estimation and long-term durability prediction for vehicular PEM fuel cell stacks under dynamic operational conditions," *IEEE Transactions on Power Electronics*, 2024. DOI: <https://doi.org/10.1109/tpel.2024.3502499>
- [20] Mei, J., Meng, X., Tang, X., Li, H., Hasanien, H., Alharbi, M., Dong, Z., Shen, J., Sun, C., Fan, F. and Jiang, J., "An accurate parameter estimation method of the voltage model for proton exchange membrane fuel cells," *Energies*, vol. 17, no. 12, p. 2917, 2024. DOI: <https://doi.org/10.3390/en17122917>
- [21] Huang, G., Zhou, Y., Yang, C., Zhu, Q., Zhou, L., Dong, X., Li, J. and Zhu, J., "Optimal allocation method of circuit breakers and switches in distribution networks considering load level variation," *Processes*, vol. 11, no. 8, p. 2235, 2023. DOI: <https://doi.org/10.3390/pr11082235>
- [22] Epifanio G. P., González J. F. V., Usberti F. L., Tarrataga L., and de Assis L. S., "Switch allocation problem in power distribution systems with distributed generation," in *Operations research forum*, 2023, vol. 4, no. 3, p. 58: Springer. DOI: <https://doi.org/10.1007/s43069-023-00236-1>
- [23] Azizi A., Vahidi B., and Nematollahi A. F., "Reconfiguration of active distribution networks equipped with soft open points considering protection constraints," *Journal of Modern Power Systems and Clean Energy*, vol. 11, no. 1, pp. 212-222, 2023. DOI: <https://doi.org/10.35833/mpce.2022.000425>

- [24] Liasi S., Ghiasi N., and Hadidi R., "Optimal switch placement to improve the reliability of distribution network in interconnected network of microgrids using a graph-based approach," *IEEE Transactions on Industry Applications*, vol. 60, no. 4, pp. 5470-5479, 2024. DOI: <https://doi.org/10.1109/tia.2024.3384355>
- [25] Khani M. and Safdarian A., "Effect of sectionalizing switches malfunction probability on optimal switches placement in distribution networks," *International Journal of Electrical Power & Energy Systems*, vol. 119, p. 105973, 2020. DOI: <https://doi.org/10.1016/j.ijepes.2020.105973>
- [26] Jooshaki M., Karimi-Arpanahi S., Lehtonen M., Millar R. J., and Fotuhi-Firuzabad M., "Electricity distribution system switch optimization under incentive reliability scheme," *IEEE Access*, vol. 8, pp. 93455-93463, 2020. DOI: <https://doi.org/10.1109/access.2020.2995374>
- [27] Žarković S. D., Shayesteh E., and Hilber P., "Integrated reliability centered distribution system planning—Cable routing and switch placement," *Energy Reports*, vol. 7, pp. 3099-3115, 2021. DOI: <https://doi.org/10.1016/j.egyr.2021.05.045>
- [28] Shahbazian A., Fereidunian A., and Manshadi S. D., "Optimal switch placement in distribution systems: A high-accuracy MILP formulation," *IEEE Transactions on Smart Grid*, vol. 11, no. 6, pp. 5009-5018, 2020. DOI: <https://doi.org/10.1109/tsg.2020.3000315>
- [29] Li B., Wei J., Liang Y., and Chen B., "Optimal placement of fault indicator and sectionalizing switch in distribution networks," *IEEE Access*, vol. 8, pp. 17619-17631, 2020. DOI: <https://doi.org/10.1109/access.2020.2968092>
- [30] Jooshaki M., Karimi-Arpanahi S., Lehtonen M., Millar R. J., and Fotuhi-Firuzabad M., "Reliability-oriented electricity distribution system switch and tie line optimization," *IEEE Access*, vol. 8, pp. 130967-130978, 2020. DOI: <https://doi.org/10.1109/access.2020.3009827>
- [31] Forcan J. and Forcan M., "Optimal placement of remote-controlled switches in distribution networks considering load forecasting," *Sustainable Energy, Grids and Networks*, vol. 30, p. 100600, 2022. DOI: <https://doi.org/10.1016/j.segan.2021.100600>
- [32] Yari A., Shakarami M., Namdari F., and Moradi CheshmehBeigi H., "A new practical approach to optimal switch placement in the presence of distributed generation," *Iranian Journal of Science and Technology, Transactions of Electrical Engineering*, vol. 44, pp. 989-1002, 2020. DOI: <https://doi.org/10.1007/s40998-019-00284-6>
- [33] Reiz C., De Lima T. D., Leite J. B., Javadi M. S., and Gouveia C. S., "A multiobjective approach for the optimal placement of protection and control devices in distribution networks with microgrids," *IEEE Access*, vol. 10, pp. 41776-41788, 2022. DOI: <https://doi.org/10.1109/access.2022.3166918>
- [34] Hajiabadi M. E., Samadi M., Lotfi H., Nikkhah M. H., Kaveh K., and Zarif M., "Optimal Placement of Protection Switches in a Real Distribution Network Based on Reliability Importance Using an Improved Gravitational Search Method," in *2023 27th International Electrical Power Distribution Networks Conference (EPDC)*, 2023, pp. 16-24: IEEE. DOI: <https://doi.org/10.1109/epdc59105.2023.10218799>
- [35] Dwivedi, D., Mitikiri, S.B., Babu, K.V.S.M., Yemula, P.K., Srinivas, V.L., Chakraborty, P. and Pal, M., "Technological advancements and innovations in enhancing resilience of electrical distribution systems," *International Journal of Critical Infrastructure Protection*, p. 100696, 2024. DOI: <https://doi.org/10.1016/j.ijcip.2024.100696>
- [36] Zaini F. A., Sulaima M. F., Razak I. A. Zulkafli W. A., N. I., and Mokhlis H., "A review on the applications of PSO-based algorithm in demand side management: challenges and opportunities," *IEEE Access*, vol. 11, pp. 53373-53400, 2023. DOI: <https://doi.org/10.1109/access.2023.3278261>

FIGURE CAPTIONS

Figure 1: Challenges Overcome by the Proposed GRIDMAP Model

Figure 2: Sample distribution grid model

Figure 3: The MIPSO Algorithm

Figure 4: Binary encoding process

Figure 5: Decision-Making Process for Candidate Point Evaluation

Figure 6: Interruption Duration Calculation for Temporary and Permanent Faults in Power Grids

Figure 7: The modified IEEE 69-bus system

Figure 8: Protective and control device quantity

TABLE CAPTIONS

Table 1: Comparison of Recent research on reliability-based switch placement

Table 2: Comparison Between Adjacency Matrix and GRIDMAP Matrices

Table 3: Metaheuristic Algorithms and Their Inspirations

Table 4: General Characteristics of Algorithms

Table 5: Parameters of IEEE 69 Bus System

Table 6: Location of Primary Devices

Table 7: Devices Placed (Scenario 1)

Table 8: Devices Placed (Scenario 2)

Table 9: Devices Placed (Scenario 3)

Table 10: Devices Placed (Scenario 4)

Table 11: Comparison of Scenarios

Table 12: Performance Comparison of Algorithms (Single Run)

Table 13: Stability Analysis of MIPSO + GRIDMAP (10 Runs)

Table 14: the effects of increasing rates Lr

Table 15: Impact of Equipment Heterogeneity on Total Cost and Computational Performance

FIGURES

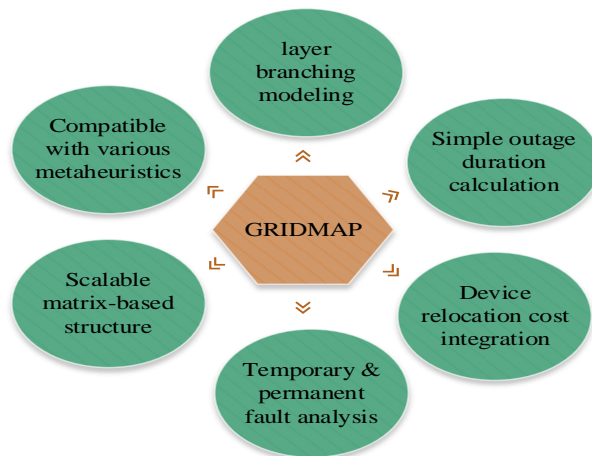


Figure 1: Challenges Overcome by the Proposed GRIDMAP Model

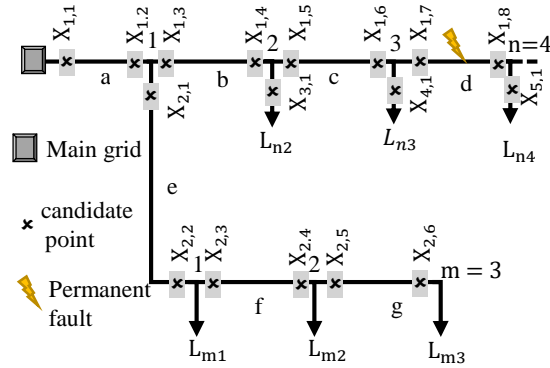


Figure 2: Sample distribution grid model

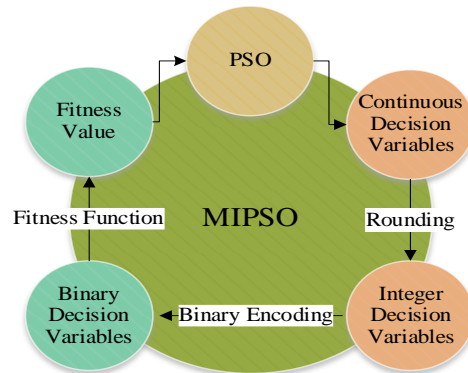


Figure 3: The MIPSO Algorithm

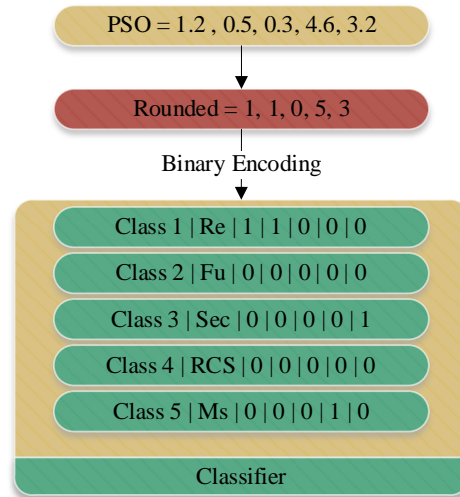


Figure 4: Binary encoding process

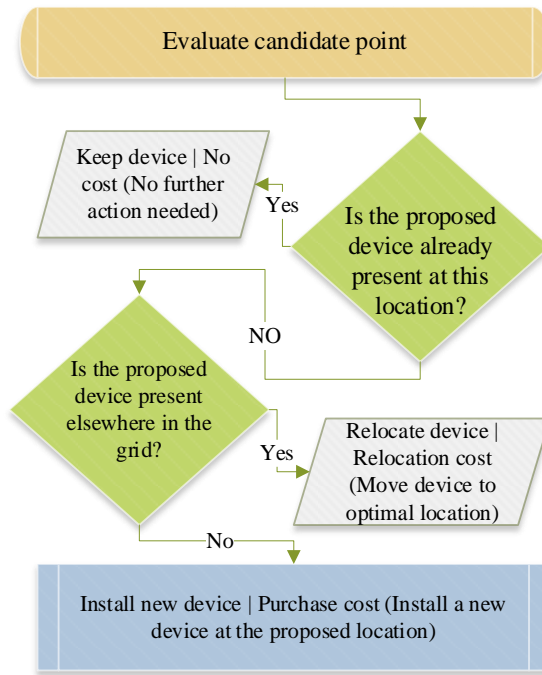


Figure 5: Decision-Making Process for Candidate Point Evaluation

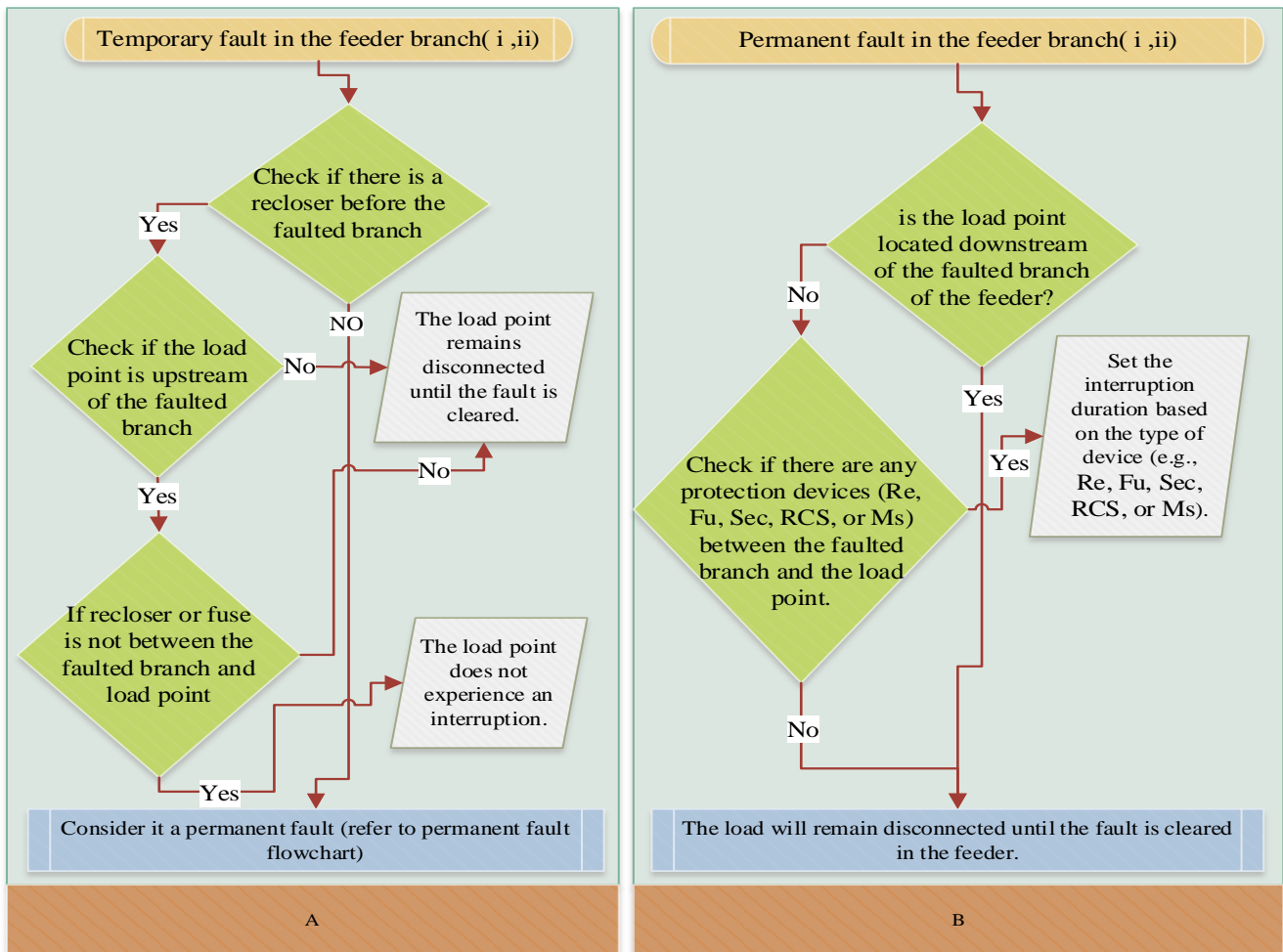


Figure 6: Interruption Duration Calculation for Temporary and Permanent Faults in Power Grids

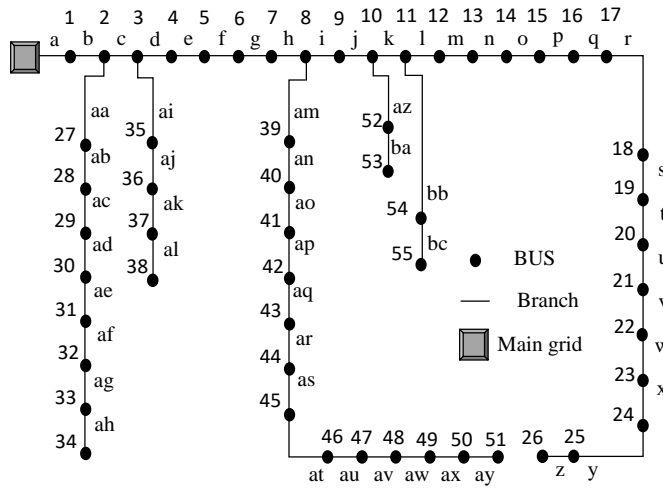


Figure 7: The modified IEEE 69-bus system

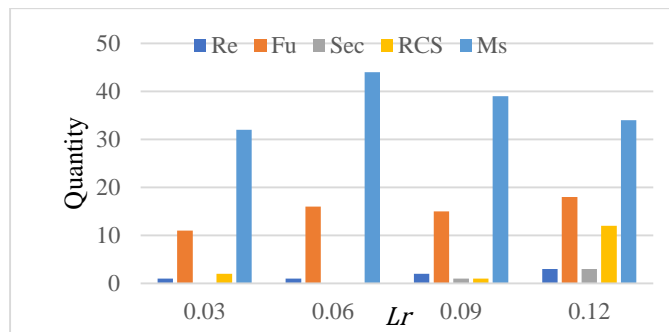


Figure 8: Protective and control device quantity

TABLES

Table 1: Comparison of Recent research on reliability-based switch placement

Article	1	2	3	4	5	6	7
[1]	✓	×	✓	✓	✓	✓	×
[27]	×	×	×	✓	✓	×	×
[28]	×	×	×	✓	✓	×	×
[29]	✓	×	×	×	×	×	×
[30]	×	×	×	✓	✓	×	×
[31]	×	×	×	✓	✓	×	×
[32]	×	×	×	✓	✓	×	×
[33]	×	×	×	✓	✓	×	×
[34]	×	×	×	✓	✓	×	✓
[35]	✓	✓	×	✓	×	×	✓
[36]	✓	×	✓	×	×	×	✓
This paper	✓	✓	✓	✓	✓	✓	✓

*Column numbers represent the following device types and features: 1- Re, 2- Fu, 3- Sec, 4- RCS, 5-MS, 6- Relocation 7- Large grid

Table 2: Comparison Between Adjacency Matrix and GRIDMAP Matrices

Feature	Adjacency Matrix	GRIDMAP Matrices
Purpose	Represent connectivity between nodes	Model grid topology, load, and equipment placement
Structure	Square ($n \times n$)	Rectangular (e.g., $n \times (m + 1)$, $2n \times (m + 1)$)
Content	Binary (0/1) or edge weights	Node attributes (loads, devices, positions)

Graph Type	Simple directed/undirected graph	Directed, hierarchical distribution grid
Interpretation	Shows if a direct connection exists	Captures position, direction, and downstream relationships
Applications	Graph algorithms (DFS, Dijkstra, etc.)	Power grid analysis, fault isolation, restoration planning

Table 3: Metaheuristic Algorithms and Their Inspirations

No.	Algorithm	Inspiration / Concept
1	Modified Particle Swarm Optimization (MIPSO)	Inspired by the collective movement of birds and fish
2	Imperialist Competitive Algorithm (ICA)	Simulates the dynamics of imperialistic competition among nations
3	Ant Colony Optimization (ACO)	Inspired by the path-finding behavior of ants

Table 4: General Characteristics of Algorithms

Feature	MIPSO	ACO	ICA
Convergence Speed	High	Low	Medium
Ease of Implementation	Simple	Complex	Moderate
Suitability for Discrete Problems	With modifications	Yes	Yes
Suitability for Continuous Problems	Yes	With modifications	Yes

Table 5: Parameters of IEEE 69 Bus System

Section Feeder			Branch information							Bus information			
			λ^P (f/y)	repair time (h) for Section Feeder							No.	load (kWh)	Type of load
a	aa	ab	0.01	a	3.6	aa	4	ab	5.8	1-3	15	R	
b	ba	bb	0.03	b	3.8	ba	4.2	bb	5.8	4-6	20	R	
c	ca	cb	0.06	c	4	ca	4.6	cb	6	7-9	15	C	
d	da	db	0.02	d	4.2	da	4.8	db	--	10-12	35	C	
e	ea	eb	0.1	e	4.4	ea	5	eb	--	13-15	45	I	
f	fa	fb	0.08	f	4.6	fa	5.2	fb	--	16-18	50	I	
g	ga	gb	0.09	g	4.8	ga	5.4	gb	--	19-21	15	R	
h	ha	hb	0.02	h	5	ha	5.8	hb	--	22-24	25	R	
i	ia	ib	0.04	i	5.2	ia	4.2	ib	--	25-27	35	I	
j	ja	jb	0.05	j	5.4	ja	4.4	jb	--	28-30	15	R	
k	ka	kb	0.1	k	5.6	ka	4.6	kb	--	31-33	20	C	
l	la	lb	0.07	l	5.8	la	4.8	lb	--	34-36	35	I	
m	ma	mb	0.03	m	6	ma	5.2	mb	--	37-39	20	R	
n	na	nb	0.02	n	6.2	na	5.4	nb	--	40-42	15	C	
o	oa	ob	0.01	o	6.4	oa	5.6	ob	--	43-45	50	I	
p	pa	pb	0.07	p	6.6	pa	5.8	pb	--	46-48	15	C	
q	qa	qb	0.02	q	6.8	qa	6	qb	--	49-51	20	R	
r	ra	rb	0.01	r	7	ra	6.2	rb	--	52-54	35	I	
s	sa	sb	0.1	s	7.2	sa	6.4	sb	--	55-57	15	C	
t	ta	tb	0.02	t	7.4	ta	6.6	tb	--	58-60	50	I	
u	ua	ub	0.07	u	7.6	ua	6.8	ub	--	61-63	20	C	
v	va	vb	0.06	v	7.2	va	7	vb	--	64-66	15	R	
w	wa	wb	0.02	w	8	wa	7.2	wb	--	--	--	--	
x	xa	xb	0.04	x	8.2	xa	7.4	xb	--	--	--	--	
y	ya	yb	0.01	y	8.4	ya	7.6	yb	--	--	--	--	
z	za	zb	0.01	z	8.6	za	5.6	zb	--	--	--	--	

Table 6: Location of Primary Devices

	NO.	Start of Branch	End of Branch
Re	0	----	----
Fu	5	q, z	as, bs, bg
Sec	1	ad	
RCS	1	bd	
MS	3	af	bh, h

Table 7: Devices Placed (Scenario 1)

	No.	Start of Branch	End of Branch
Re	1	b	
Fu	11	aa, c, ai, am, as, at, j, s, v	aq, ba
Sec	0	----	----
RCS	2	bb, p	----
MS	32	ab, ad, af, ah, f, h, an, au, ax, i, ba, l, n, o, q, r, z	ae, aj, ak, al, e, ao, ap, ar, as, aw, k, bc, s, t, y

Table 8: Devices Placed (Scenario 2)

	No.	Start of Branch	End of Branch
Re	1	b	
Fu	11	aa, ai, d, am, i, l	as, at, aw, az, r
Sec	0	----	----
RCS	0	----	----
MS	32	ab, aj, ak, f, at, au, ay, ba, k, p, r, t, z	ag, ah, d, h, am, an, ap, ar, j, bb, bc, l, m, o, s, u, v, x, y

Table 9: Devices Placed (Scenario 3)

	No.	Start of Branch	End of Branch
Re	1	a	----
Fu	15	aa, ae, af, ai, aj, e, h, am, at, i, ba, k, bc, n, z	----
Sec	0	----	----
RCS	1	p	----
MS	18	ab, ah, c, al, d, f, ap, as, au, j, bb, o, q, s, u, w, x, y	----

Table 10: Devices Placed (Scenario 4)

	No.	Start of Branch	End of Branch
Re	1	----	a
Fu	12	----	b, ab, c, ai, d, an, as, i, ba, k, m, r
Sec	0	----	----
RCS	1	----	t
MS	17	----	aa, ac, ad, ak, e, am, ao, ap, aq, ar, at, aw, bb, l, o, q, y

Table 11: Comparison of Scenarios

Scenario	Total Cost (\$)	C^P (\$)	C^T (\$)	C^{eq} (\$)	Time to Solve (s)
1	628,270	508,370	1,145	118,760	1,452
2	609,840	507,980	1,084	100,780	1,246
3	587,580	497,390	630	89,830	1,285
4	698,500	619,900	1,134	80,461	1,098

Table 12: Performance Comparison of Algorithms (Single Run)

Algorithm	Total Cost (\$)	C^P (\$)	C^T (\$)	C^{eq} (\$)	Time to Solve (s)
PSO	628,270	508,370	1,145	118,760	1,452
ACO	650,805	525,780	1,325	123,700	2,821
ICA	640,541	515,463	1,278	123,800	2,112

Table 13: Stability Analysis of MIPSO + GRIDMAP (10 Runs)

Run	Time to Solve (s)	C^{eq} (\$)	C^T (\$)	C^P (\$)	Total Cost (\$)
1	622,000	502,000	12,500	107,500	1,350
2	625,500	503,800	12,700	109,000	1,360
3	626,300	507,900	12,600	105,800	1,480
4	628,700	508,200	12,550	107,950	1,455
5	617,200	501,500	12,650	103,050	1,448
6	622,900	505,800	12,580	104,520	1,370
7	621,400	502,100	12,530	106,770	1,460
8	622,600	504,300	12,620	105,680	1,452
9	623,100	507,100	12,540	103,460	1,435
10	617,000	502,700	12,590	101,710	1,430

Table 14: the effects of increasing rates Lr

Lr	Total Cost (\$)	C^P (\$)	C^T (\$)	C^{eq} (\$)	Time to Solve (s)
0.03	628,270	508,370	1,145	118,760	1,452
0.06	741,070	592,190	1,311	147,570	1,439
0.09	877,650	724,190	1,559	151,900	1,435
0.12	1,097,000	868,520	1,984	226,510	1,338

Table 15: Impact of Equipment Heterogeneity on Total Cost and Computational Performance

Scenario	Total Cost (\$)	C^{eq} (\$)	C^T (\$)	C^P (\$)	Type 1 Quantity	Type 2 Quantity	Type 3 Quantity	Solution Time (s)
1	636,210	120,760	12,080	503,370	48	0	0	1,420
2	642,710	125,850	12,520	504,340	39	5	0	3,830
3	645,000	127,730	12,620	504,650	38	4	2	7,950

BIOGRAPHIES



Mehdi Mohammadian Mehr received a Bachelor's degree in Electrical Engineering, specializing in Power Systems, from Shahid Chamran University of Ahvaz, from 2018 to 2022. He then pursued a Master's degree in Electrical Engineering with a concentration in Power Systems at the same university, from 2022 to 2024. His academic background emphasizes energy systems, particularly in the areas of renewable energy integration, smart grids, and advanced forecasting techniques. His research interests include the application of artificial intelligence in power system optimization, distribution network design and enhancement, electric load forecasting and control, power system reliability and resilience, and the integration of energy storage and renewable energy resources into power grids.



Hossein Farzin received the BSc and PhD degrees in Electrical Engineering from Sharif University of Technology, Tehran, Iran, in 2011 and 2016, respectively. He was a postdoctoral researcher at Sharif University of Technology, from 2016 to 2017. He is currently an Associate Professor in the Electrical Engineering Department, Shahid Chamran University of Ahvaz, Ahvaz, Iran. His research interests include microgrids design and optimization, integration of distributed energy resources and electric vehicles in smart grid, and power system reliability and resilience. Dr. Farzin ranked 2nd in Iran's nationwide universities entrance exam in 2007, and is ranked among the world's top 2% most cited researchers in 2021 and 2023. He has authored more than 60 journal and conference papers, and serves as an editor of the Scientia Iranica journal.